Thermoreversible Gelation Driven by Coil-to-Helix Transition of Polymers

Fumihiko Tanaka

Department of Polymer Chemistry, Graduate School of Engineering, Kyoto University, Kyoto 606-8501 Japan

Received November 15, 2002; Revised Manuscript Received April 21, 2003

ABSTRACT: This paper theoretically studies thermoreversible gelation driven by aggregation of helices formed on the polymer chains. Two fundamentally different cases of (i) multiple association of single helices, and (ii) association by multiple helices with multiplicity k (such as double helices ($k = 2$), triple helices ($k = 3$), etc.) are treated on the basis of different equations. The helix length distribution on a polymer chain (or assemble of chains for multiple helices) is derived as a function of polymer concentration and temperature. It obeys a power law of the parameter $t = 1 - \nu/(1 - \theta)$, where θ is the helix content per chain and ν is the average number of helices on a chain divided by the total number n of the repeat units. The sol/gel transition point is found on the temperature−concentration plane. It is found that, in the case of k-ple helices, the condition $n\theta/\bar{\xi} = k/(k - 1)$ is fulfilled at the gel point, where $\bar{\xi}$ is the average helix length. Hence, the independent measurement of θ and $\bar{\xi}$ gives the multiplicity k. Theoretical calculation of the total helix content in the solution is compared with experimental data of optical rotation in ι-carrageenan solutions at different polymer concentrations. It is shown that at low temperature there is a sharp transition from network to bundle state (pair, triplet, etc.). This network-to-bundle transition becomes a real phase transition in the limit of infinite chain length.

1. Introduction

The properties of biopolymer gels and networks have been the subject of a great deal of work by many researchers.[1−6] One of the main problems studied so far is the molecular mechanism of cross-linking in thermoreversible gelation of biological polymers such as polysaccharides and proteins. These cross-links mostly involve physical bonds rather than covalent ones. The complications introduced by physical bonds, or segment association, are such that main three attractive interactions, i.e., hydrogen bonding, hydrophobic interaction, and electrostatic interaction, all simultaneously set in when biopolymers are cross-linked. Further complication appears with the fact that most biopolymers undergo conformational transitions preceding gelation. Activation of the particular functional groups on a polymer chain accompanied by a proper three-dimensional conformation change is a necessary prerequisite for the interchain cross-linking. For instance, water-soluble natural polymers such as gelatin and polysaccharides (agar, alginate, carrageenan, gellan, etc.) change their conformation from the random coil state to a partially helical state, and then the helical parts aggregate to form extended network junctions.[1,2,4−10] In our recent study,[11] we developed statistical-mechanical theory for the study of gelation strongly coupled to polymer conformational transitions. In this paper, we refine our theoretical treatment by focusing on the interplay between helix formation and cross-linking in aqueous solutions of polysaccharides. To avoid complexity, we consider mainly the hydrogen bonding in forming helices (followed by their hydrophobic aggregation) and neglect the polyelectrolyte effect.

Since the physical properties such as helix content, length distribution of junction zones, elastic modulus, etc. strongly depend on the thermal history of the sample solutions,[12] we first introduce two time scales: a time scale for helix formation and that for helix aggregation.

Let us first consider the case where the helix formation is faster than the association. The helices formed after the solution is quenched from the high-temperature uniform liquid state quickly reach almost equilibrium length, and then, by further adjustment during the lapse of time, associate with each other into junctions of the true equilibrium length that minimizes the free energy of the network as a whole. If the solution is slowly annealed (at a rate slower than helix association), on the other hand, the equilibrium network structure at a given temperature is not the one formed at the earlier stage, so that polymers try to adjust their helix length and spatial distribution of junction zones to reach the true equilibrium from the *wrong initial conditions*. The topological constraints introduced in the network in the preceding stage is so strong that the network continues to change but can never reach equilibrium. The random coils connecting the network junctions get tenser as they are pulled from the junctions, and as a result, the modulus continues to increase.[12]

Recently, a similar separable two-step mechanism of gelation through coil-to-helix transition was confirmed for synthetic polymers with stereo-regularity.[13−15] It was found that, in solutions of syndiotactic poly(methyl methacrylate) in toluene, a fast intramolecular conformational change is followed by an intermolecular association leading eventually to gelation.

Let us next consider the more complex case where the rate of helix growth and that of helix association are comparable. Kinetics of the network formation becomes more complex, because helices start to aggregate as soon as they are nucleated. The spatial distribution of junctions becomes far from the equilibrium one, and the solution never reaches equilibrium. The system shows intrinsically nonequilibrium time development with

10.1021/ma021688y CCC: $25.00
Published on Web 06/10/2003

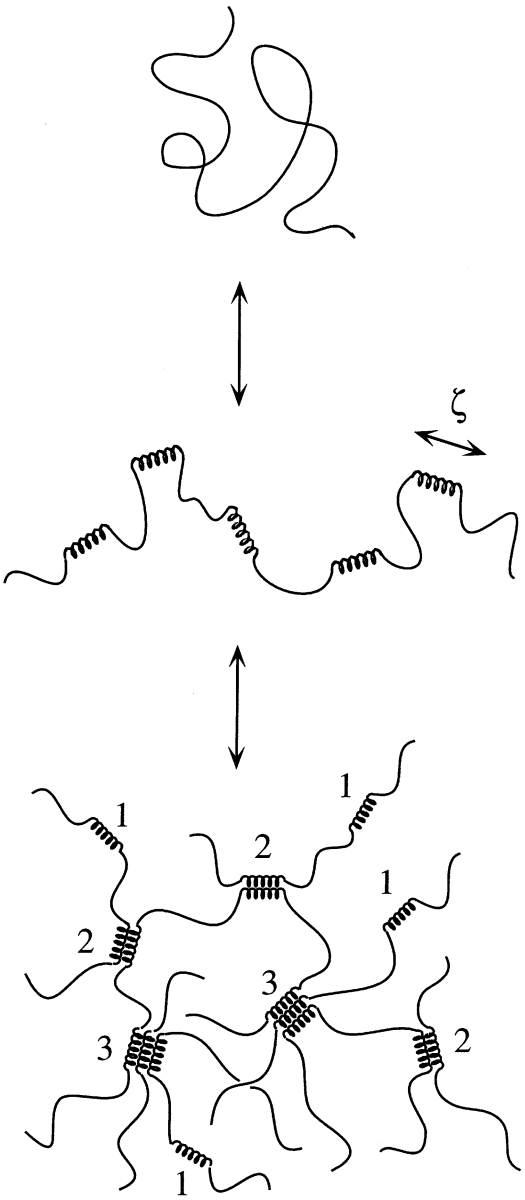

Figure 1. Thermoreversible gelation in helix-forming polymer solutions. In the case of multiple association of single helices, polymers form partial helices of variable length ζ upon cooling, and helices aggregate into network junctions with multiplicity indicated by the figures.

strong topological constraints, so that studies from kinetic viewpoint are necessary.[12,16,17]

In this paper, we focus on the simpler case of separable time scales. Kinetic studies on the more complex case of nonseparable time scales will be reported elsewhere.

2. Model Polymer Solutions

We consider model polymer solutions in which polymers in random-coil conformation (reference conformation) at a given temperature and concentration first form partial helices after being cooled, and then helices aggregate into multiple junctions (Figure 1).

The multiplicity of a junction is defined by the number of helices combined to it. Therefore, it is 1 for unassociated helices, 2 for pairwise junctions, and 3 for triple junction etc. If a chain carries many short helices, its functionality (number of functional groups) is high, but association energy is small because short helices are not strongly bound to each other. On the other hand, if a chain carries a small number of long helices, its functionality is low, but the association energy is large. Therefore, there is a competition between helix growth and helix association. This competition is described by the relative magnitude of the following two parameters. The first one is the probability

$$\eta_\zeta(T) \equiv \exp(-\Delta A_\zeta/k_B T) \tag{2.1}$$

for the formation of a helix of length ζ, where ΔA_ζ is the free energy of a helix measured relative to the reference conformation (random coil). The other one is the association constant

$$\lambda_\zeta(T) \equiv \exp(-\Delta f_\zeta/k_B T) \tag{2.2}$$

where Δf_ζ is the free energy change when a helix of length ζ is bound into a junction. In the following study, we assume that the time scale of helix growth is sufficiently fast compared to that of the helix association, so that helix distribution on a chain reaches almost equilibrium before association. After association sets in, each junction zone adjusts its length in order for the entire solution to reach equilibrium.

Before getting into the theory, we first distinguish two fundamentally different cases, i.e., multiple association of single helices and association by multiple helices (Figure 2). These are fundamentally different in the following points:

- Unassociated helices remain in the networks in the single-helix case, while there are no isolated helices in multiple-helix case. In the former case, the unassociated helices do not serve as network junctions, so that helix content is not necessarily proportional to the elastic modulus of the network.
- There is a perfect size matching among the sequence length joining in a junction in multiple-helix case by its definition, while small helices may associate with the longer ones in the single-helix case. The helix length in a junction is therefore not necessarily uniform in the latter.
- Two neighboring helices on the same chain may merge into one when they grow in the single-helix case, while they collide and will not merge in the multiple-helix case.

In most biopolymer gels, experimental distinction between pairwise association of single helices and intertwined double helices has been impossible, so that the more general term "*helical dimer*" was used in the literature.[7,8] In what follows, we treat them in a different way, but, to avoid unnecessary complexity, we assume *perfect size matching* of helices in the case of single helix when they associate. In other words, helices of different length are regarded as different functional groups.

Let us consider more about the double-helix case (Figure 3). In addition to the double helices formed in biopolymers such as κ-carrageenan, gellan, etc., we can include in the same category other types of junction zones such as hydrogen-bonded ladder type junctions as seen in polyacid−polybase complexes,[18] and association by forming stereocomplex egg-box junction zones[20,38] in which metallic ions are captured. (Small loops (defects) in the ladder can also be taken into consideration, but they are excluded in the present study.) For such pairwise association of polymer chains, Higgs and Ball[9] in their pioneering work theoretically suggested

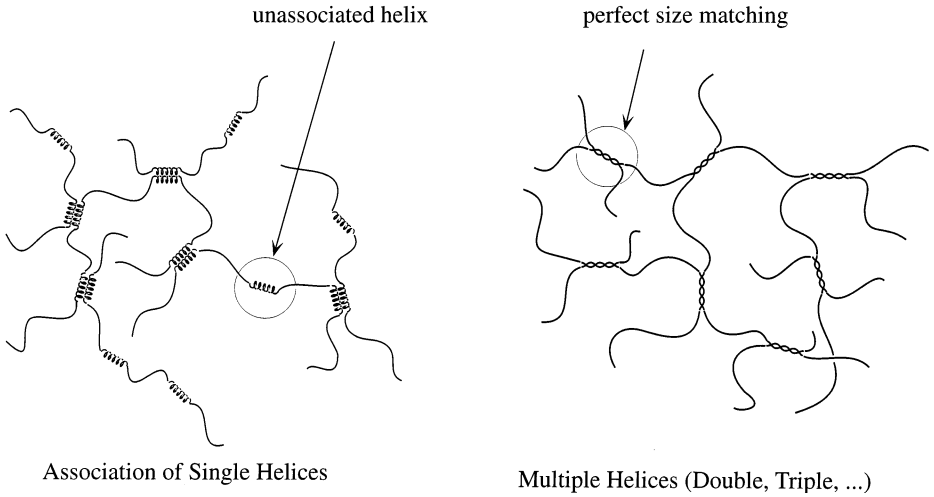

Figure 2. Two fundamentally different types of networks cross-linked by helices: (left) multiple association of single helices, and (right) association by multiple helices.

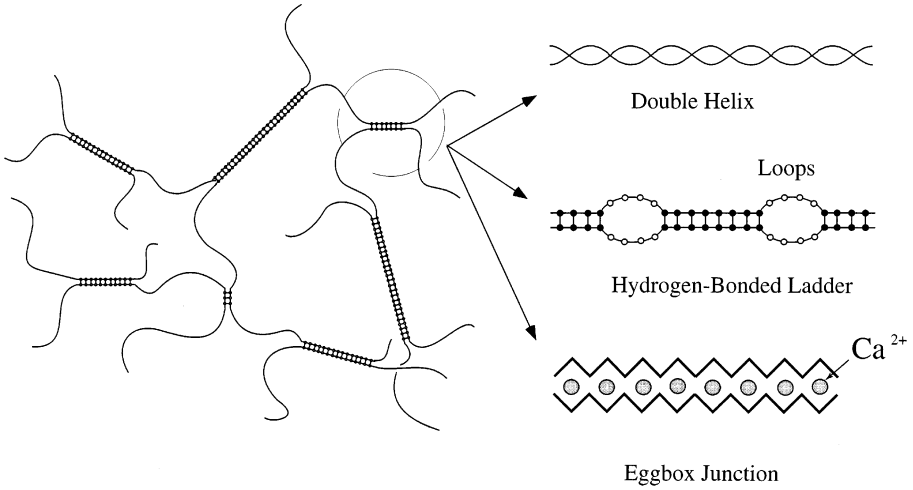

Figure 3. Three examples of zipper type junction zones: double helix, hydrogen-bonded ladder (with small loops), and egg-box junction.

the occurrence of *pairing transition* where the mean length of bonded sequences reaches the total polymer chain length. We will study this transition in detail by new statistical−mechanical method treating association of many chains.

3. Distribution Function of Helices

Let us first briefly review the single-chain coil-to-helix transition problem. From the late 1950s, many papers in the literature studied this problem.[21] Most of them employed either matrix method or generating function method, but they are useless for many-chain problems. We therefore here reformulate the problem by employing the combinatorial counting method. Our new method can easily be extended to suit many-chain problems.

Consider a polymer chain carrying the total number n of statistical units (Figure 4). In order for helices to be generated on this chain, helix sequences must be selected from the finite length n. Let j_ζ be the number of helices with length $\zeta = 1, 2, 3, ..., n$ (counted in terms of the statistical units). Then, the number of different ways to select $j \equiv \{j_1, j_2, j_3, ...\}$ is given by

$$\omega(\{j\}) = \frac{(n - \sum \zeta j_\zeta)!}{(\prod j_\zeta!)(n - \sum \zeta j_\zeta - \sum j_\zeta)!} \qquad (3.1)$$

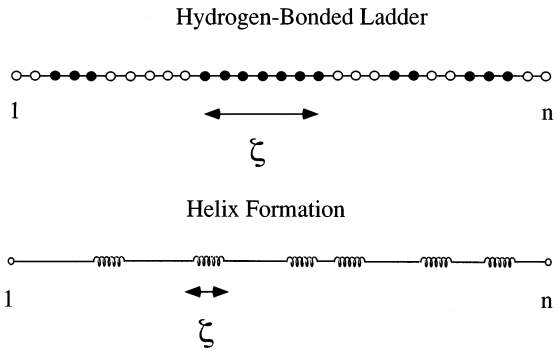

Figure 4. Sequence selection in the hydrogen-bonding ladder (top) and helix formation (bottom). The number j_ζ of ζ-sequences are selected from the finite total length n.

Detailed derivation of this combinatorial factor is given in Appendix A.

The free energy of a chain with the distribution j of helices measured relative to the random-coil conformation is then given by

$$\exp[-\beta F_{\text{single}}(j)] = \omega(j) \prod_\zeta \eta_\zeta^{j_\zeta} \qquad (3.2)$$

where η_ζ is the statistical weight (eq 2.1) for a helix of

length ζ. To find the most probable distribution of helices, we minimize the free energy F_{single} by changing j and find

$$j_\zeta/n = (1 - \theta - \nu)\eta_\zeta t^\zeta \tag{3.3}$$

Here,

$$\theta \equiv \sum_{\zeta=1}^{n} \zeta j_\zeta/n \tag{3.4}$$

is the helix content (number of statistical units in the helices divided by the total number of units), and

$$\nu \equiv \sum_{\zeta=1}^{n} j_\zeta/n \tag{3.5}$$

is the number of helices on the chain (divided by the total number of units). The parameter t is defined by

$$t \equiv (1 - \theta - \nu)/(1 - \theta) \tag{3.6}$$

The physical meaning of this parameter is the probability for a randomly chosen monomer to be in the random-coil sequence. Substituting the distribution (eq 3.3) into these definitions, we find

$$\theta = tV_1(t)/[1 + tV_1(t)] \tag{3.7}$$

and

$$\nu = tV_0(t)/[1 + tV_1(t)] \tag{3.8}$$

where functions $V(x)$ are defined by

$$V_0(x) \equiv \sum_{\zeta=1}^{n} \eta_\zeta x^\zeta \tag{3.9a}$$

$$V_1(x) \equiv \sum_{\zeta=1}^{n} \zeta\eta_\zeta x^\zeta \tag{3.9b}$$

By definition (eq 3.6), the parameter t must satisfy the equation

$$\frac{t}{1 - t} V_0(t) = 1 \tag{3.10}$$

This is the same equation as that found by Zimm and Bragg[22] (referred to as ZB) and also by Lifson and Roig.[23] ZB employed the form

$$\eta_\zeta = \sigma_1 s(T)^\zeta \tag{3.11}$$

for the statistical weight of a helix, where σ_1 is the helix initiation factor, and $\ln s(T) = \text{constant} - \epsilon_H/k_BT$ with ϵ_H (<0) being the hydrogen bonding energy between the nearest monomers (amino residues in proteins). We then have

$$V_0(t) = \sigma_1 s t w_0(st) \tag{3.12a}$$

$$V_1(t) = \sigma_1 s t w_1(st) \tag{3.12b}$$

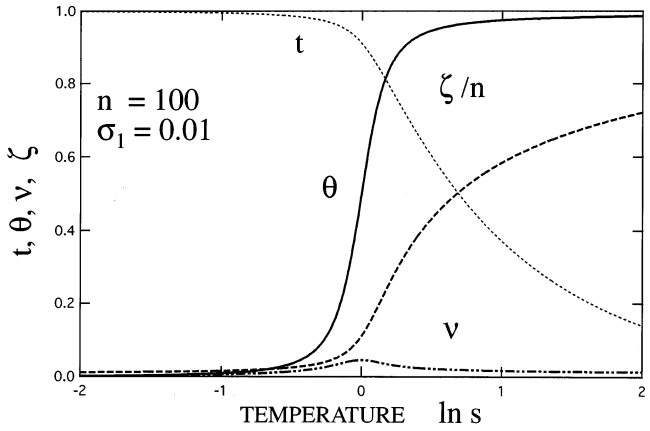

Figure 5. Helix content θ (—), number of helices ν (— ·· —), mean helix length $\bar{\zeta}$ (— —), and the probability t (- -) for a randomly chosen monomer to belong to the random coil part shown as functions of the temperature. Temperature is measure in terms of $\ln s = \text{const} + |\epsilon_H|/k_BT$ by using the probability s of hydrogen-bond formation.

where the functions w_0 and w_1 are defined by

$$w_0(x) \equiv \sum_{\zeta=1}^{n} x^{\zeta-1} \tag{3.13a}$$

$$w_1(x) \equiv \sum_{\zeta=1}^{n} \zeta x^{\zeta-1} \tag{3.13b}$$

Lifson and Roig[23] used a slightly different weight

$$\eta_\zeta = \nu \quad (\text{for } \zeta = 1), \qquad \nu^2 w^{\zeta-2} \quad (\text{for } \zeta \geq 2) \tag{3.14}$$

The result does not differ so much, so that, in the following study, we employ the simpler ZB weight. Figure 5 plots t, θ, ν and the mean helix length $\bar{\zeta} \equiv \theta/\nu$ as functions of the temperature. Temperature is measured in terms of $\ln s$. The coil-to-helix transition takes place at around $\ln s = 0$. The helix initiation parameter σ_1 should be small for the transition to be sharp. The transition becomes sharper with molecular weight and becomes a real phase transition in the limit of infinite chain length.

4. Free Energy of the Solution

Let us move onto the many-chain problem. In a solution at a given polymer volume fraction ϕ and temperature T, polymer chains carry helices whose length distribution is given by j_ζ. This distribution is decided by the minimization of the *total free energy of the solution*, and it depends on ϕ as well as T. A polymer chain is regarded as a functional molecule carrying j_ζ of functional groups distinguished by the length ζ of helices (Figure 6).

We now have the problem of thermoreversible gelation of polydisperse molecules carrying different species of functional groups capable of forming junctions of variable multiplicity. We have recently studied thermoreversible gelation of functional molecules (carrying a single species of functional group) whose functionality is not a fixed number but varies depending on the temperature.[11] The present problem is an extension of our previous study to the case of many species of functional groups. Therefore, we can find the free energy of the solution by repeating the same theoretical consideration on the basis of the lattice theory of polymer solution[24−27] combined with Flory−Stockmayer branch-

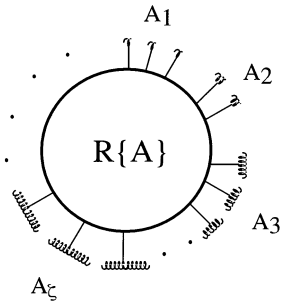

Figure 6. Schematic picture of a functional molecule carrying different species of functional groups A_1, A_2, ...

ing theory[28−31] of gelation. We are then led to

$$\beta\Delta F/\Omega = f_{FH}(\phi) + f_{AS}(\phi) \tag{4.1}$$

for the free energy per lattice cell (Ω is the total number of lattice cells in the solution), where

$$f_{FH}(\phi) \equiv \frac{\phi}{n}\ln\phi + (1-\phi)\ln(1-\phi) + \chi\phi(1-\phi) \tag{4.2}$$

is the Flory−Huggins free energy in the absence of association, and

$$f_{AS}(\phi) \equiv \frac{\phi}{n}\ln\left(\frac{\phi_\lambda}{\phi}\right) + \sum_\zeta \frac{1}{\lambda_\zeta}\int_0^{z_\zeta} z u'(z)\, dz \tag{4.3}$$

is the free energy due to the conformational change and association.[11] Here, ϕ_λ is the volume fraction of "λ molecules", i.e., polymers that remain in the reference conformation (random coil for the present study) indicated by subscript λ. The temperature-dependent parameter $\lambda_\zeta(T)$ is the association constant (eq 2.2) for helices of length ζ. A brief derivation of this free energy is given in Appendix B. The parameter z_ζ is related to the polymer volume fraction through the equation[11,32,33]

$$\lambda_\zeta < j_\zeta > \phi/n = z_\zeta u(z_\zeta) \tag{4.4}$$

The volume fraction of λ molecules relative to the total volume fraction is given by[11]

$$\phi_\lambda/\phi = \exp[-\ln F_{\{0\}}(\{z\})] \tag{4.5}$$

where the moments of helix distribution are defined by

$$F_{\{m\}}(\{z\}) \equiv \sum_{j\neq 0}\left(\prod_\zeta j_\zeta^{m_\zeta}\right)[u(z_\zeta)^{j_\zeta}]\omega(\{j\})\prod_\zeta \eta_\zeta^{j_\zeta} \tag{4.6}$$

Here, $\{m\}$ is the set of integers $\{m_1, m_2, ...\}$ that indicate the powers of the moment. The average helix number is, for example, given by

$$\langle j_\zeta\rangle = F_{\{0,0,...,1,0,0,...\}}(\{z\})/F_{\{0,0,0,...\}}(\{z\}) \tag{4.7}$$

where the ζth number in $\{m\}$ in the numerator is unity.

The function $u(z)$ is the junction function for giving a correct statistical weight to each multiplicity[31,33] and is given by

$$u(z) = \sum_{k\geq 1}\gamma_k z^{k-1} \tag{4.8}$$

For instance, it is

$$u(z) = 1 + z^{k-1} \tag{4.9}$$

for k-ple association of single helices and

$$u(z) = z^{k-1} \tag{4.10}$$

for association by k-ple helices. (The first term for $k = 1$ does not exist in the latter because there is no isolated helix.)

Let us next minimize this free energy by changing the helix distribution function j to find the most probable one. After a detailed calculation of the condition $\delta(\beta\Delta F/\Omega)/\delta j_\zeta = 0$, we find in Appendix C

$$j_\zeta/n = (1-\theta-\nu)\eta_\zeta u(z_\zeta)t^\zeta \tag{4.11}$$

where parameter t is defined by relation 3.6 as before, but now it depends on the polymer concentration. Distribution function j can also be written as

$$j_\zeta/n = (1-\theta)\eta_\zeta u(z_\zeta)t^{\zeta+1} \tag{4.12}$$

Comparing this result with the single-chain helix distribution (eq 3.3), we find that interchain association is included in the front factor junction function $u(z)$. The parameter z_ζ is related to the polymer concentration by eq 4.4, which now produces the relation

$$z_\zeta = (1-\theta)\phi\lambda_\zeta\eta_\zeta t^{\zeta+1} \tag{4.13}$$

for the most probable distribution found above. Upon substitution of the junction function (eq 4.8) for $u(z)$ into the distribution function, we find that the helix content θ per chain is given by

$$\theta = \sum_{k\geq 1}\theta_k \tag{4.14}$$

and the number of helices ν per chain by

$$\nu = \sum_{k\geq 1}\nu_k \tag{4.15}$$

where

$$\theta_k \equiv \gamma_k(1-\theta)t\sum_{\zeta=1}^{n}\zeta\eta_\zeta z_\zeta^{k-1}t^\zeta \tag{4.16}$$

is the content of helices participating in the junctions of multiplicity k, and

$$\nu_k \equiv \gamma_k(1-\theta)t\sum_{\zeta=1}^{n}\eta_\zeta z_\zeta^{k-1}t^\zeta \tag{4.17}$$

is the number of helices participating in them. In particular for the unassociated helices (in the single-helix case), we have

$$\theta_1 = (1-\theta)tV_1(t) \tag{4.18}$$

and

$$\nu_1 = (1-\theta)tV_0(t) \tag{4.19}$$

where V_0 and V_1 are defined by eq 3.12. From the relation (eq 4.13) for z, the above results are expressed

as

$$\theta_k = \gamma_k(1-\theta)t[(1-\theta)\phi t]^{k-1}W_1^{(k)}(t^k) \quad (4.20)$$

$$\nu_k = \gamma_k(1-\theta)t[(1-\theta)\phi t]^{k-1}W_0^{(k)}(t^k) \quad (4.21)$$

where new functions W s are defined by

$$W_0^{(k)}(x) \equiv \sum_{\zeta=1}^{n} \lambda_\zeta{}^{k-1}\eta_\zeta{}^k x^\zeta \quad (4.22a)$$

$$W_1^{(k)}(x) \equiv \sum_{\zeta=1}^{n} \zeta\lambda_\zeta{}^{k-1}\eta_\zeta{}^k x^\zeta \quad (4.22b)$$

In particular, for $k = 1$, we have $W_0^{(1)}(x) = V_0(x)$ and $W_1^{(1)}(x) = V_1(x)$. The average helix length of the junction with multiplicity k is then given by

$$\bar{\xi}_k \equiv \theta_k/\nu_k = W_1^{(k)}(t^k)/W_0^{(k)}(t^k) \quad (4.23)$$

The parameter t is then given by

$$t = 1 - t\sum_{k\geq 1}\gamma_k\{[(1-\theta)\phi t]^{k-1}W_0^{(k)}(t^k)\} \quad (4.24)$$

To find the equation for t, we now solve eq 4.14 with respect to $1-\theta$ in terms of t, and substitute the result into eq 4.24. The equation takes the form

$$\frac{t}{1-t}\{V_0(t) + \sum_{k\geq 2}\gamma_k[(1-\theta)\phi t]^{k-1}W_0^{(k)}(t^k)\} = 1 \quad (4.25)$$

(Further elimination of θ from this equation requires the models of junctions.) This is the extension of the ZB condition (eq 3.10) to the many-chain problems.

Let us now examine physical meaning of the parameter t. We start with the relation (eq 4.5) for the volume fraction of chains in random-coil conformation relative to the total polymer volume fraction, and substitute the most probable distribution (eq 4.12) for j_ζ into this equation. Asymptotic evaluation then leads to

$$\ln F_{\{0\}}(\{z\}) = n(1-\theta)\ln(1-\theta) - n(1-\theta-\nu)\times \ln(1-\theta-\nu) - \sum_{\zeta=1}^{n} j_\zeta\{\ln(1-\theta-\nu) + \zeta\ln t\} \quad (4.26)$$

$$= -n\ln t$$

Hence, we have

$$\phi_\lambda/\phi = t^n \quad (4.27)$$

Therefore, the parameter t gives the probability for a randomly chosen monomer on a chain to be a member of a random-coil sequence.

5. Gel Point

In this section, we find the condition for the gel point where solution turns from sol state into gel state. The gel point here is defined by the percolation point where the largest cluster in the solution spans the entire system, i.e., where the three-dimensional macroscopic network appears. This point can be found by the condition such that the weight-average molecular weight of the clusters diverges. For the model polyfunctional molecules carrying f_i functional groups of the i-species capable of forming multiple junctions *only within the same species*, the gel point is shown in Appendix D to be given by

$$1/\bar{\mu}_w + 1/\sum_i f_i - 1 = 0 \quad (5.1)$$

where the weight-average junction multiplicity $\bar{\mu}_w$ is defined by the reciprocal average

$$1/\bar{\mu}_w \equiv \sum_i (f_i/\bar{\mu}_{w,i})/\sum f_i \quad (5.2)$$

In the present helix problem, the suffix i specifies the length ζ of a helix, and f_i corresponds to the number j_ζ of helices on a chain. Since the average multiplicity for the helices of length ζ is given by[33]

$$\bar{\mu}_\zeta = 1 + z_\zeta u'(z_\zeta)/u(z_\zeta) \quad (5.3)$$

the condition for the gel point is given by

$$\sum_{\zeta=1}^{n} \frac{u(z_\zeta)}{u(z_\zeta)+z_\zeta u'(z_\zeta)} j_\zeta = n\nu - 1 \quad (5.4)$$

For association by multiple helices, the junction function takes the form $u(z) = z^{k-1}$, so that the gel point condition takes a particularly simple form

$$n\nu_k = k/(k-1) \quad (5.5)$$

Since ν_k is given by the helix content θ divided by the average helix length $\bar{\zeta}$, we can find the multiplicity k by independent measurement of θ and $\bar{\zeta}$. In particular, $n\theta/\bar{\zeta} = 2$ for the double helices ($k = 2$) and $n\theta/\bar{\zeta} = 1.5$ for the triple helices ($k = 3$). It is between 1.5 and 2 if double and triple helices are mixed. Thus, we conclude that, for polymers in the solution to percolate, the number of helices, irrespective of their length, should exceed a critical value. The elastic modulus near above the percolation point depends therefore directly on the number of junctions rather than the total helix content.

For multiple (k-ple) association of single helices, the junction function is given by $u(z) = 1 + z^{k-1}$, so that the gel point condition becomes

$$\sum_{\zeta=1}^{n} \frac{z_\zeta{}^{k-1}}{1 + kz_\zeta{}^{k-1}} j_\zeta = \frac{1}{k-1} \quad (5.6)$$

6. Solution Properties

To study phase separation, thermodynamic stability, osmotic pressure and other properties, we have to know the chemical potentials of all species in the solution. To obtain the chemical potential of the solvent molecule and λ molecules, we take the derivatives of the free energy with respect to the number N_0 and N_λ, and find them in the general forms[11]

$$\beta\Delta\mu_0 = 1 + \ln(1-\phi) - \nu^S + \chi\phi^2 - [\sum_f \delta'_f(\phi)\nu_f^G]\phi \quad (6.1a)$$

$$\beta\Delta\mu_\lambda/n = (1+\ln\phi_\lambda)/n - \nu^S + \chi(1-\phi)^2 + [\sum_f \delta'_f(\phi)\nu_f^G](1-\phi) \quad (6.1b)$$

where

$$\nu^{S} \equiv 1 - \phi + \sum_{\mathbf{j},\mathbf{l}} \nu(\mathbf{j};\mathbf{l}) \tag{6.2}$$

is the total number density of particles and clusters that possess translational degree of freedom. (Note that it is not related to the number of helices although the same letter ν is used.) The last term in these chemical potentials comes from the gel part in the postgel regime. The function $\delta_f(\phi)$ is the free energy for binding one functional group into the gel network, and ν_f^{G} the number density of the polymer chains with functionality f in the gel network (see ref 11 for more details). They are important only in the postgel regime. The number density ν^{S} is shown in Appendix B to be given by

$$\nu^{S} = 1 - \phi + \frac{\phi}{n} - \sum_{\zeta} \frac{1}{\lambda_\zeta} \int_0^{z_\zeta} z u'(z)\, dz \tag{6.3}$$

so that the chemical potentials are explicitly given by

$$\frac{\beta\Delta\mu_\lambda}{n} = \frac{1}{n}\ln\phi + \left(1 - \frac{1}{n}\right)\phi + \chi(1-\phi)^2 + \ln t + \phi\sum_{k\geq 2}\frac{k'}{k}\nu_k \tag{6.4a}$$

$$\beta\Delta\mu_0 = \ln(1-\phi) + \left(1 - \frac{1}{n}\right)\phi + \chi\phi^2 + \phi\sum_{k\geq 2}\frac{k'}{k}\nu_k \tag{6.4b}$$

in the pregel regime.

We next expand the solvent chemical potential in powers of the polymer volume fraction and find

$$A_2 = \frac{1}{2} - \chi - \frac{1}{2}t_0^{\,2} W_0^{(2)}(t_0^{\,2}) \tag{6.5}$$

for the second virial coefficient ($\gamma_2 = 1$ by definition). Here, t_0 is the solution of eq 4.24 with vanishing polymer concentration $\phi = 0$. Since the function $W_0^{(2)}$ is positive by its definition, pairwise association of single helices, or formation of double helices, reduces the second virial coefficient. As we will see below, there is a temperature at which the average helix length reaches the entire chain length ("*pairing transition*"). This transition becomes sharper with increase in the polymer molecular weight and becomes a true phase transition in the limit of infinite chain length. The second virial coefficient negatively diverges at this limit of sharp pairing transition.

By differentiating the chemical potentials, the thermodynamic stability limit, or spinodal condition, is found to be given by

$$\frac{1}{n\phi} + \frac{1}{1-\phi} - 2\chi + \frac{\partial(\ln t)}{\partial\phi} = 0 \tag{6.6}$$

Since $\partial t/\partial\phi < 0$, the possibility of phase separation in athermal solvent ($\chi = 0$) remains. Detailed study of these solution properties will be reported in a forthcoming paper.

7. Association by Multiple Helices

We first study formation of multiple helices with a fixed multiplicity k. For such k-ple helices, we have

$$u(z) = z^{k'} \tag{7.1}$$

where the abbreviation $k' \equiv k - 1$ has been used. The fundamental equations are then given by

$$j_\zeta/n = (1-\theta)^k t^k \phi^{k'} \lambda_\zeta^{\,k'} \eta_\zeta^{\,k} (t^k)^\zeta \tag{7.2}$$

for the helix distribution function and

$$\theta = (1-\theta)^k \phi^{k'} t^k W_1^{(k)}(t^k) \tag{7.3}$$

$$\nu = (1-\theta)^k \phi^{k'} t^k W_0^{(k)}(t^k) \tag{7.4}$$

for the helix content per chain and the number of helices per chain. (Suffix k is omitted since $\theta_k = \theta$ and $\nu_k = \nu$.) The equation for t takes the form

$$(1-t)[1 + \bar{\zeta}(t)(1-t)]^{k'} = \phi^{k'} t^k W_0^{(k)}(t^k) \tag{7.5}$$

where the average helix length is given by eq 4.23. The gel point is given by the condition $n\nu = k/k'$ or

$$n\theta/\bar{\zeta}(t) = k/k' \tag{7.6}$$

so that independent measurement of θ and $\bar{\zeta}$ at the gel point gives the helix multiplicity.

Let us focus our study on double helices in this paper. More complex triple helices and mixtures of double and triple helices will be studied in a separate paper. We have for $k = 2$

$$\theta = (1-\theta)^2 \phi t^2 W_1^{(2)}(t^2) \tag{7.7}$$

and

$$\nu = (1-\theta)^2 \phi t^2 W_0^{(2)}(t^2) \tag{7.8}$$

For the statistical weight of a double helix with sequence length ζ, we assume ZB form

$$\eta_\zeta = 1 \quad \text{and} \quad \lambda_\zeta = \sigma_2 \lambda(T)^\zeta \tag{7.9}$$

The first equation ensures that a chain does not form helices by itself. The second equation gives the weight σ_2 for the initiation (nucleation) of a double helix, i.e., the probability for an arbitrarily chosen pair of monomers on different chains to start winding. This is the counterpart of σ_1 for a single chain to nucleate helices. The latter is expected to be small, but σ_2 can be order unity if there is no strict restriction on monomer conformation in starting chain winding. The weight $\lambda(T)$ is associated with a monomer belonging to a helix. This weight comes from the hydrogen bond between the monomer pair in a helix and can be regarded as the association constant. It is written as

$$\ln\lambda(T) = \Delta s/k_B - \epsilon_A/k_B T \tag{7.10}$$

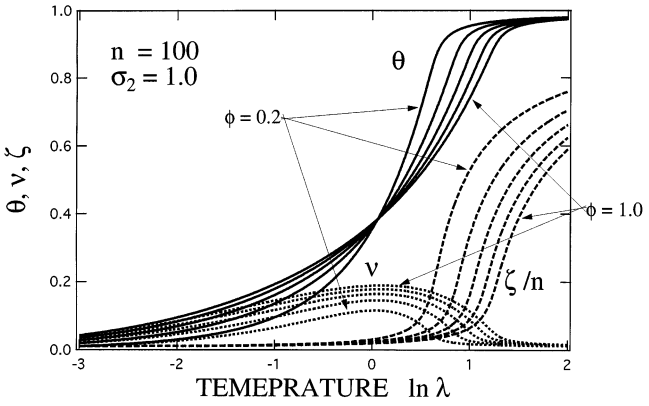

Figure 7. Helix content θ (—), number of helices ν (- -), mean helix length $\bar{\xi}$ per chain (— —) shown as functions of the temperature. Temperature is measured in terms of $\ln \lambda = \text{const} + |\epsilon_A|/k_BT$ by using the association constant λ per monomer. Polymer volume fraction is changed from curve to curve. The total DP of a polymer is fixed at $n = 100$. The helix initiation factor is fixed at $\sigma_2 = 1.0$. With increase in the polymer concentration, the helix number increases, while the mean helix length decreases.

in terms of the entropy and enthalpy of association. We then have

$$W_0^{(2)}(t^2) = \sigma_2{}^2\lambda t^2 w_0(\lambda t^2) \tag{7.11a}$$

$$W_1^{(2)}(t^2) = \sigma_2{}^2\lambda t^2 w_1(\lambda t^2) \tag{7.11b}$$

where functions w_0 and w_1 are defined by eq 3.13. The equation for t becomes

$$(1 - t)\{1 + w_1(\lambda t^2)(1 - t)/w_0(\lambda t^2)\} = \sigma_2\lambda\phi t^4 w_0(\lambda t^2) \tag{7.12}$$

In the limit of infinite dilution, we have the solution $t_0 = 1$. At finite concentration, t is monotonically decreases as temperature is lowered.

Figure 7 shows helix content, number of helices, and average helix length as functions of the temperature for polymers carrying $n = 100$ repeat units. The temperature is measured in terms of $\ln \lambda \sim |\epsilon_A|/k_BT$. The polymer volume fraction is changed from curve to curve. The coil-to-helix transition takes place at around $\ln \lambda = 0$, and slightly shifts to higher temperature with the polymer concentration. The helix initiation parameter is fixed at $\sigma_2 = 1.0$ by assuming the simplest case where there is no restriction for a pair of chains to start winding. At high temperatures, helix content increases with polymer concentration, but at low temperatures it decreases because θ is defined by the total number of repeat units in helices on a single chain. To obtain the total helix content in the solution, the number of polymer chains must be multiplied to θ. This total content of helices in the solution is an increasing function of the polymer concentration at all temperature regions. It is expected to be proportional to the rotation angle of the polarization plane in optical measurements.

Near around the transition temperature, many short helices are nucleated. At low temperatures, helices grow longer and longer, so that there are only few long helices on a chain. For instance, their length reaches about 80% at $\ln \lambda = 2$. The double helices with 80% long are practically rodlike rigid pairs of polymers. Hence they form various anisotropic liquid-crystalline mesophases.[34−36] However, the study of such mesophases is beyond the scope of the present paper. The average helix length decreases with polymer concentration at low-temperature region.

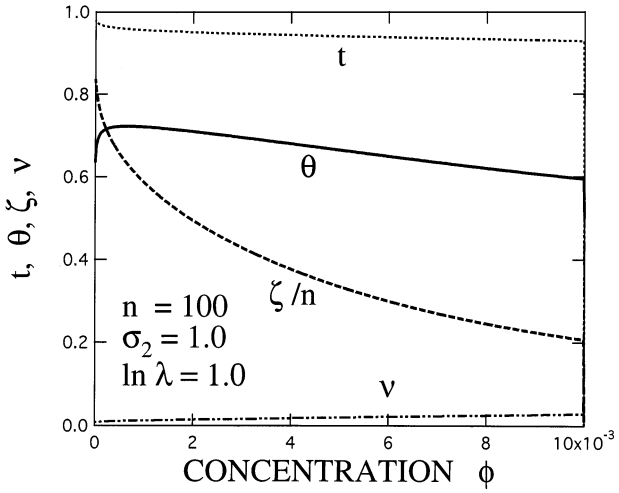

Figure 8. Concentration profile of θ (—), ν (— ·· —), $\bar{\xi}$ (— —) and t (- -). The peak in the helix content θ is located in the extremely dilute regime, so that separation of a double helix into two isolate chains is practically impossible.

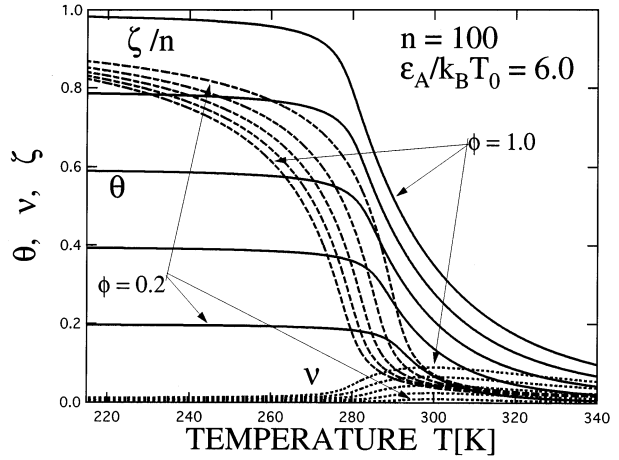

Figure 9. Total content $\theta \times \phi$ of helices (—), ν (- -), and $\bar{\xi}$ (— —) plotted against the absolute temperature.

To see this in more detail, we show in Figure 8 the concentration profile of these quantities at a fixed temperature $\ln \lambda = 1.0$. Helices monotonically grow by dilution, but there is a peak in θ, because at zero concentration θ must vanish by definition of double helix. The concentration at which θ shows a peak is extremely small and shift toward $\phi = 0$ with increase in the polymer molecular weight. Therefore, it is practically impossible to separate pairs into isolate chains by simple dilution.

To compare the results with optical measurements, Figure 9 plots the same quantities as functions of the absolute temperature. Parameters are arbitrarily chosen to take an overview of the behavior such that the transition temperature is given by $T = 290$ K and association energy by $|\epsilon_A|/k_BT = 6.0$.

Figure 10 compares the experimentally measured optical rotation angle for the degraded ι-carrageenan aqueous solution with 0.1 mol of added salt[37] with theoretically calculated total helix content in the solution. The molecular distribution of degraded carrageenan was measured in the experiment and the average chain length was estimated to be 47 residues. The

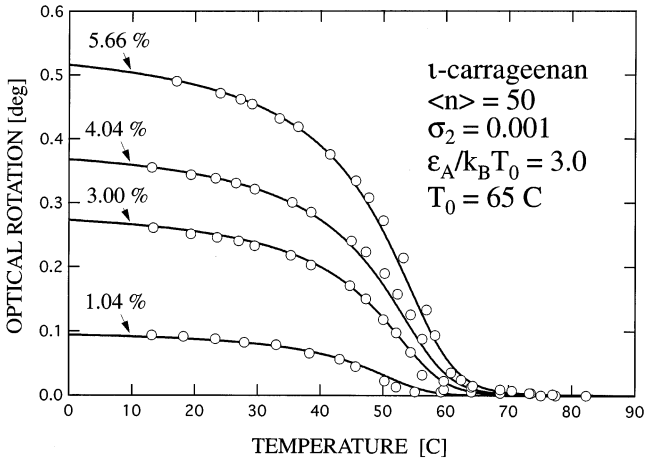

Figure 10. Comparison of the experimentally measured optical rotation angles (○) and theoretically calculated total content of helices in a solution (—). Experimental data were obtained from degraded ι-carrageenan solution with 0.1 mol salt. Polymer concentration is varied from curve to curve. The proportionality constant between theoretical helix content and optical rotation is found from the data at the highest concentration of 5.66% measured.

optical rotation was measured at four concentrations by changing the temperature. The ι-carrageenan with such a small molecular weight (47 residues) does not form gels in this temperature−concentration region. DSC measurement on cooling and heating process in the same temperature range was also carried out together with optical measurement. The result on cooling and on heating did not show any significant difference, and gave a unique value for the enthalpy of coil-to-helix transition. Therefore, the solution was treated as in thermal equilibrium. Since the problem of whether ι-carrageenan, without Ca^{2+} ions, exists in double helix[7,8,38] or in paired single helix[39,40] at the junctions has not been resolved at this moment, we attempted to fit the data by assuming double helix as in the experiment.[37]

The proportionality constant between theoretical helix content and optical rotation is found by fitting the data at the highest concentration of 5.66% measured. Then, theoretical results at other concentrations automatically fit the experimental data with high accuracy. It turned out that, for $\langle n \rangle = 50$, the helix initiation parameter σ_2 should be as small as 0.001 to obtain a good fit. One of the main reason ι-carrageenan does not form gels is the smallness of this helix initiation probability. The coil-to-helix transition temperature at dilute limit is fixed at $T_0 = 65$ °C.

Figure 11 summarizes the theoretical results for $n = 100$ polymers in the form of phase diagram. Solid line shows sol/gel transition line as decided by the condition (eq 7.6) for $k = 2$. Broken lines show the contours with a constant helix length. Along the rightmost one, for example, double-helices have average length $\bar{\zeta}/n = 0.8$. The sol/gel transition concentration is not a monotonic function of the temperature but turns back into high concentration at low temperatures. Helices grow so long at such low concentrations that the number of network junctions become insufficient for gelation. The phase plane is roughly divided into four regions: sol region with separate chains at high-temperature dilute regime, gel region with type I networks at high-temperature side of the postgel regime, gel region with type II networks at low-temperature side of the postgel regime, and

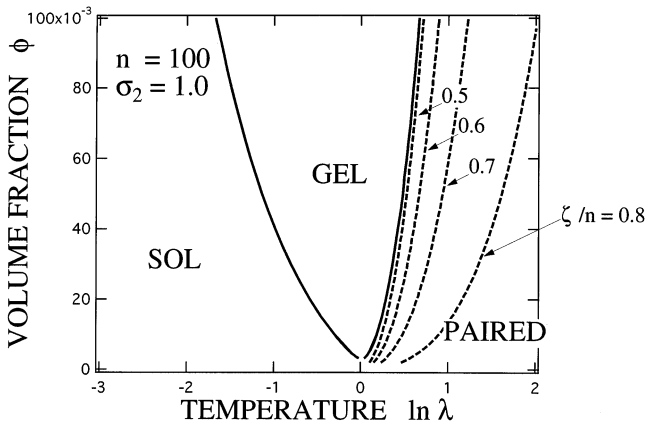

Figure 11. Temperature−concentration phase diagram of a polymer solution forming networks by double helices. The solid line shows sol/gel transition line. The dashed lines show the contour along which the average helix length takes a fixed value. At low temperatures, there is a change from network phase to pairing phase.

pairing region at low-temperature dilute regime. This is an expected phase diagram under the condition that helices grow much faster than they associate to each other. When a solution at a given concentration with separate chains at high temperature is quenched to a given temperature, the phase shown in this phase diagram is reached at equilibrium. If we further anneal the system, helices grow under a fixed given topological constraints, and show behavior different from the one shown in this equilibrium phase diagram. The growth rate $\partial\bar{\xi}/\partial T$ in this annealing process can be directly measurable through the change in the elastic modulus.

Figure 12 shows the same diagram as in Figure 7 but for a longer polymer chains. The transition becomes sharper with increase in the molecular weight. In particular, the bend in curves of θ at a low temperature becomes sharper and sharper, and eventually reveals discontinuity at infinite molecular weight. This temperature is the temperature where the transition from type II networks to pairing state becomes a real thermodynamic phase transition. It is determined by the condition $1 - \lambda t^2 = 0$ in addition to the equation for t (eq 7.12). Since $t_0 = 1$ for the dilute limit, the second virial coefficient is given by

$$A_2 = \frac{1}{2} - \chi - \frac{1}{2}\sigma_2\lambda\frac{1-\lambda^n}{1-\lambda} \qquad (7.13)$$

so that the network-to-bundle transition condition leads to negative divergence of the second virial coefficient.

Figure 13 shows the molecular weight dependence of the sol/gel transition line. The upper branch of the transition line significantly shifts to high temperature and low concentration region, but the lower branch remains at almost the same position. Such a general tendency was predicted by Higgs and Ball[9] by a simple kinetic analysis in which the helix initiation parameter (σ_2 in our notation) is simply assumed to be proportional to the polymer concentration. It is justified by the present more precise calculation on the basis of the equilibrium statistical mechanics.

8. Multiple Association of Single Helices

Let us proceed to multiple association of single helices. For simplicity, we assume monodisperse association with a fixed multiplicity k, so that we have $u(z) = 1 +$

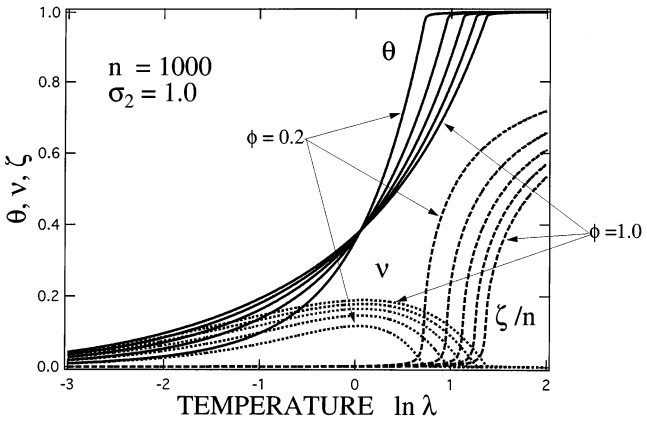

Figure 12. Same as Figure 7 but for longer chains $n = 1000$. The slope in θ around network-to-pair transition changes more abruptly. In the limit of infinitely long chains, the slope becomes discontinuous.

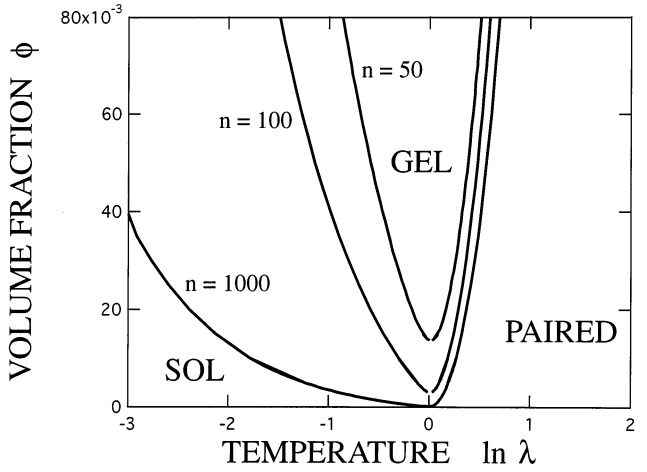

Figure 13. Sol/gel transition lines for three different molecular weight polymers. The upper branch largely shifts to higher temperature with n, but lower branch changes only little.

z^{k-1}. We also assume the perfect size matching in association. The helix distribution function then takes the same form (eq 4.12), but the junction function is given by

$$u(z_\zeta) = 1 + [(1-\theta)\phi t]^{k-1}(\lambda_\zeta \eta_\zeta t^\zeta)^{k-1} \tag{8.1}$$

The helix content and number of helices are then decomposed into two terms

$$\nu = \nu_1 + \nu_k \tag{8.2}$$

$$\theta = \theta_1 + \theta_k \tag{8.3}$$

where

$$\nu_1 = (1-\theta)tV_0(t) \tag{8.4}$$

and

$$\theta_1 = (1-\theta)tV_1(t) \tag{8.5}$$

are those of the single helices that remain unassociated in the clusters and networks. On the other hand,

$$\nu_k = (1-\theta)^k \phi^{k-1} t^k W_0^{(k)}(t^k) \tag{8.6}$$

and

$$\theta_k = (1-\theta)^k \phi^{k-1} t^k W_1^{(k)}(t^k) \tag{8.7}$$

are those of the helices in the junctions of multiplicity k. Existence of the first terms in ν and θ discriminates single helices from multiple helices. The equation for t takes the form

$$[1 - t - tV_0(t)]\{1 + tV_1(t) + \bar{\zeta}_k(t)[1 - t - tV_0(t)]\}^{k-1} = \phi^{k-1} t^k W_0^{(k)}(t^k) \tag{8.8}$$

Before getting into the detailed analysis of association of single helices, let us first take the limit of infinite dilution. By taking the limit $\phi \to 0$ in eq 8.8, we find that t satisfies

$$\frac{t}{1-t} V_0(t) = 1 \tag{8.9}$$

This is the equation derived by ZB, and also by Lifson and Roig, for the single-chain coil-to-helix transition problem. For example, we have the root

$$t_0 = \frac{1}{2s(1-\sigma_1)}\{1 + s - \sqrt{(1-s)^2 + 4\sigma_1 s}\} \tag{8.10}$$

for ZB weight. We thus confirm that our solution of the many-helix problem is a straightforward extension of the old studies to finite polymer concentrations.

In what follows we focus on the pairwise association, and employ the simplest ZB weight

$$\eta_\zeta = \sigma_1 s(T)^\zeta \tag{8.11}$$

for the helix formation, and the weight

$$\lambda_\zeta = \sigma_2 \lambda(T)^\zeta \tag{8.12}$$

for the association of helices. Then functions of our concern take the following forms:

$$V_0(t) = \sigma_1 s t w_0(st) \tag{8.13a}$$

$$V_1(t) = \sigma_1 s t w_1(st) \tag{8.13b}$$

and

$$W_0^{(2)}(t^2) = \sigma_2{}^2 \tilde{\lambda} t^2 w_0(\tilde{\lambda} t^2) \tag{8.14a}$$

$$W_1^{(2)}(t^2) = \sigma_2{}^2 \tilde{\lambda} t^2 w_1(\tilde{\lambda} t^2) \tag{8.14b}$$

by using the functions w_0 and w_1, where abbreviated notations

$$\sigma \equiv \sigma_2 \sigma_1{}^2, \text{ and } \tilde{\lambda} \equiv \lambda s^2 \tag{8.15}$$

have been used. The association constant is assumed to take the form

$$\lambda(T) = \lambda_0 s(T)^\gamma \tag{8.16}$$

Here, λ_0 is a constant and $\gamma \equiv \epsilon_A/\epsilon_H$ is the ratio between association energy ϵ_A relative to the nearest-neighbor hydrogen-bonding energy ϵ_H for helix formation.

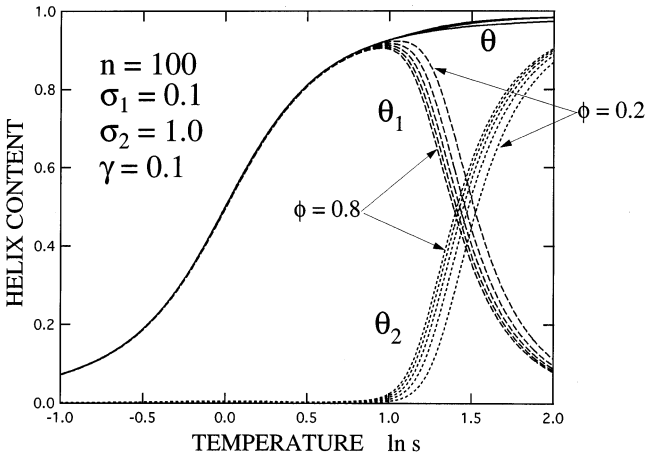

Figure 14. Content of isolated helices θ_1 (− −) and of paired helices θ_2 (--), together with their sum (—), plotted against the temperature in the weak association case ($\gamma = 0.1$). Polymer concentration is changed from curve to curve.

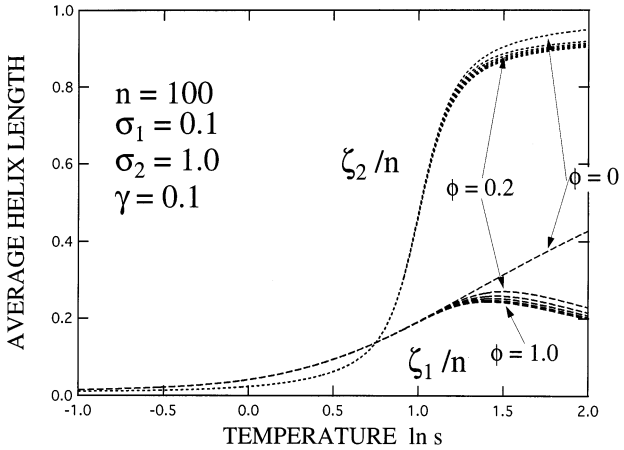

Figure 15. Average helix length $\bar{\xi}_1$ of isolated helices (− −) and $\bar{\xi}_2$ of paired helices (- -) plotted against temperature in the weak association case ($\gamma = 0.1$). Polymer concentration is changed from curve to curve.

8.1. Weak Association. We first consider the weak association case ($\gamma \ll 1$). Figure 14 shows helix contents as functions of temperature for $\gamma = 0.1$ for polymers with $n = 100$.

Figure 15 shows the average helix length. The helix initiation factor is fixed at $\sigma_1 = 0.1$ and $\sigma_2 = 1.0$ so that we have $\sigma = 0.01$. The polymer volume fraction is changed from curve to curve. The total helix content behaves like the double helix case, but its decomposition into the unassociated one θ_1 and the associated one θ_2 shows a complex variation. At high temperature, most of helices are short and unassociated. As we approach the coil-to-helix transition temperature, helices grow and association starts to take place. Elastic modulus of the network in this region is not related to the total helix content. Pair formation is sharply accelerated at the temperature around ln $s = 1.0$, and paired helices dominate below ln $s = 1.5$. Networks formed around this temperature are basically type II in which short unassociated helices (20% of the total length) are connected by long paired helices (70% of the total length) at junctions via short random coils. However, below this temperature, helices condense into long paired ones; the system becomes a concentrated solution of rodlike molecules of helix pairs. In all cases, the helix content and helix length depend only weakly on the concentration. For larger values of σ_2, the concentration dependence is enhanced. The curve for infinite dilution ($\phi = 0$) shows a different behavior from other curves at finite concentrations because of the absence of association.

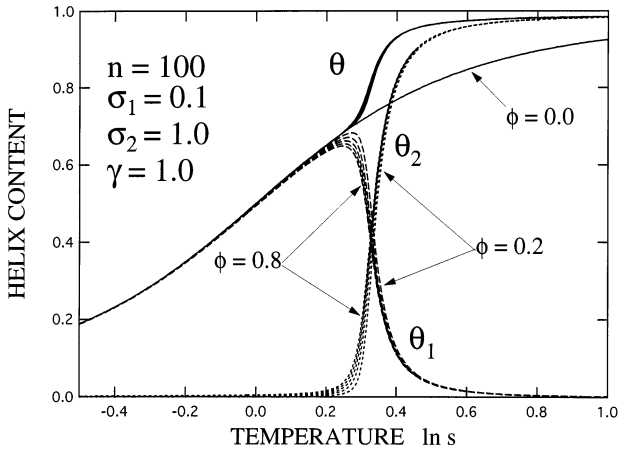

Figure 16. Same as in Figure 14 but for the strong association case ($\gamma = 1.0$).

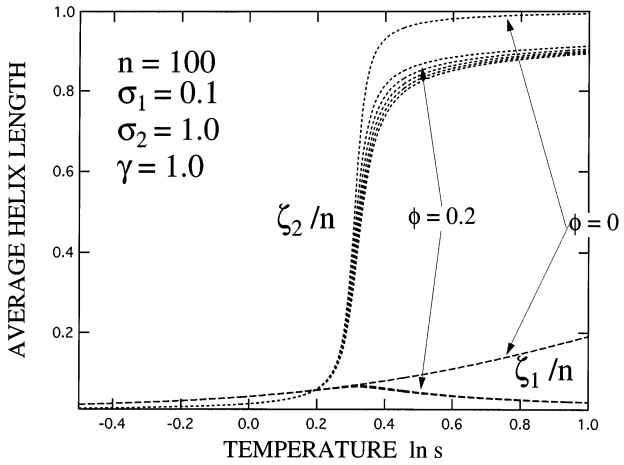

Figure 17. Same as in Figure 15 but for the strong association case ($\gamma = 1.0$).

8.2. Strong Association. We next consider the strong association case ($\gamma \geq 1$). Figure 16 shows helix contents as functions of temperature for $\gamma = 1.0$ for polymers with $n = 100$.

Figure 17 shows the average helix length. Although γ is of order unity, effect of association sets in very sharply at small values of s around ln $s = 0.2$. There is a sharp rise in θ_2 where the total helix content $\theta = \theta_1 + \theta_2$ shows a a sudden increase (except infinite dilution $\phi \rightarrow 0$). We have type I networks just above this temperature, but they disappear below ln $s = 0.4$. In the special case of $\phi \rightarrow 0$, all curves reduce to those given by ZB theory.

9. Conclusions and Discussion

We have theoretically studied coil-to-helix transitions at finite polymer concentrations and thermoreversible gelation induced by the association of helices on the basis of classical tree statistics combined with lattice theory of polymer solutions. A general criterion of the gel point is found for association by multiple helices and for multiple association of single helices. In particular for double helices, the gel point condition takes a particularly simple form $n\theta/\bar{\xi} = 2$, so that independent measurement of the helix content θ and average helix

length $\bar{\zeta}$ gives a possibility to identify the gel point. It is shown that there are two fundamentally different types of networks, i.e., networks in which random coils are cross-linked by short helices (type I) and networks in which long rodlike double helices are connected by short random coils (type II). Their elastic moduli behave differently as functions of the temperature. We have confirmed a very good agreement between our theoretical calculations of the helix content at finite concentrations and the experimental data on the optical rotation angle in ι-carrageenan solutions. It is also suggested that there is a network-to-bundle transition at a low temperature. For double helices, this transition is a "pairing transition". This transition becomes a true phase transition in the limit of infinite polymer molecular weight. Further application of the present theory to helix forming biopolymers, together with calculations of material properties such as osmotic pressure, viscosity, elastic moduli, and phase equilibria will be reported in forthcoming papers.

Our theoretical analysis is entirely based on the mean-field approximation. It employs Flory−Huggins theory for solutions and Flory−Stockmayer theory for gelation. Both are mean-field theory, and their combination is well balanced to each other in the level of approximation. As far as concentration fluctuations are concerned, the limitation of the mean-field theory can be estimated by the simple Ginzburg-Landau criterion. Let us arbitrarily select one chain in the solution, and count the average number P of polymer chains lying inside the spherical region of the radius of gyration surrounding the chain.[44] The number is given by $P \simeq \phi R^3/na^3 \simeq n^{1/2}\phi$ if there is no association. It must be sufficiently larger than unity for the mean-field approximation to be varied. If there is association, DP of the primary polymer must be replaced by the average P_w. However, if the effect of concentration fluctuations is considered beyond the mean-field approximation, the principle of equal reactivity (and also tree approximation) breaks down. Therefore, we must improve the theoretical treatment of gelation in accordance with the fluctuation theory. Consideration of small loops is relatively easy,[45] but large-scale cycles in the network are difficult to treat. Improvement of the theory along this line will therefore encounter serious difficulties.

Appendix A. Combinatorial Factor

Let us count the number of different ways to choose j_ζ sequences of the length ζ from the total finite length n. To distinguish the neighboring helices, we assume that there should be at least one monomer between them. We first imagine that helices are contracted into one statistical unit. The total length is reduced to be $n' = n - \sum\zeta j_\zeta$. The number of ways to choose $\sum j_\zeta$ units from n' is given by $n'!/(\sum j_\zeta!)(n' - \sum j_\zeta)!$, but since we cannot distinguish the states which are obtained by replacing helices of the same length, we have to multiply the factor $(\sum j_\zeta)!/(\Pi j_\zeta!)$. We are thus led to the result $\omega(\{j\})$ given in eq 3.1. Selection of segment sequences with uniform length from the finite total length was first discussed by Gornick and Jackson[41] to study crystallization of polymers.

Appendix B. Free Energy of the Solution

We start from the chemical potentials (eq 6.1) that was found in our previous work.[11] Gibbs−Duhem's relation then gives the free energy per lattice site in the form

$$\beta\Delta F/\Omega = f_{FH}(\phi) + f_{AS}(\phi) \tag{B1}$$

where $f_{FH}(\phi)$ is the Flory−Huggins part and

$$f_{AS}(\phi) = \frac{\phi}{n}\ln\left(\frac{\phi_\lambda}{\phi}\right) + \frac{\phi}{n} + (1-\phi) - \nu^S \tag{B2}$$

is due to the effect of association.

The last four terms give the loss in the translational degree of freedom due to association of polymer chains. It is given by

$$\frac{\phi}{n} + (1-\phi) - \nu^S = \frac{\phi}{n} - \sum_{\mathbf{j},\mathbf{l}}\nu(\mathbf{j};\mathbf{l}) = \frac{\phi}{n}\left(1 - \frac{1}{P_n}\right) \tag{B3}$$

by using the number-average degree of polymerization P_n. The number-average is usually calculated on the basis of stoichiometric consideration, and it is shown in Appendix D to be given by

$$\frac{\phi}{n}(1 - 1/P_n) = \sum_\zeta \frac{1}{\lambda_\zeta}\int_0^{z_\zeta} zu'(z)\,dz \tag{B4}$$

Appendix C. Helix Distribution Function

We now minimize the above free energy by changing j_ζ:

$$\frac{\delta}{\delta j_\zeta}(\beta\Delta F/\Omega) = -\frac{\phi}{n}\left[-\zeta\ln(n - \sum\zeta j_\zeta) - \ln j_\zeta + (\zeta-1)\ln(n - \sum\zeta j_\zeta - \sum j_\zeta) + \ln[\eta_\zeta u(z_\zeta)] + \sum_{\zeta'}\frac{j_{\zeta'}}{u(z_{\zeta'})}\frac{\delta u(z_{\zeta'})}{\delta j_{\zeta'}}\right] + \frac{\delta}{\delta j_\zeta}\sum_{\zeta'}\frac{1}{\lambda_{\zeta'}}\int_0^{z_\zeta} zu'(z)\,dz = 0 \tag{C1}$$

The last term gives

$$\frac{\delta}{\delta j_\zeta}\sum_{\zeta'}\frac{1}{\lambda_{\zeta'}}\int_0^{z_\zeta} zu'(z)\,dz = \frac{1}{\lambda_{\zeta'}} z_\zeta u'(z_\zeta)\frac{\delta z_\zeta}{\delta j_\zeta} \tag{C2}$$

but by taking the derivative of eq 4.4, this term turns out to cancel the last term in the parentheses in eq C1. Thus, we find

$$-\zeta\ln(n - \sum\zeta j_\zeta) - \ln j_\zeta + (\zeta-1)\ln(n - \sum\zeta j_\zeta - \sum j_\zeta) + \ln[\eta_\zeta u(z_\zeta)] = 0 \tag{C3}$$

This gives the helix distribution function eq 4.11.

Appendix D. Conditions for the Gel Point

In this appendix, we derive the number-average and weight-average molecular weight of the functional molecules $R\{A_i\}$ carrying the number f_i of the functional group A_i specified by the index i. Each functional group is assumed to form junctions of arbitrary multiplicity *within the same species* (Figure 6).

The number-average molecular weight can be derived by simple stoichiometric consideration. We first consider pairwise association. Since one degree of translational freedom is lost every time one bond is formed between a pair of functional groups, the total number of clusters

moving independently in the solution is given by

$$N - \frac{1}{2}\sum_i \alpha_i f_i N \tag{D1}$$

where N is the number of $R\{A_i\}$ molecules and α_i is the degree of association of species A_i, i.e., the probability for a group A_i to be associated. The factor $^1/_2$ in front is necessary to correct overcounting a bond twice. Hence the number-average is given by

$$P_n^{-1} = 1 - \frac{1}{2}\sum_i f_i \alpha_i \tag{D2}$$

For the multiple association, we first introduce the probability $p_k^{(i)}$ for an arbitrarily chosen A_i group to be associated into the junction of multiplicity k. Then, the total number of clusters moving independently in the solution can be expressed as

$$N - \sum_i f_i N \sum_{k\geq 1} \frac{k-1}{k} p_k^{(i)} = N - \sum_i \left(1 - \frac{1}{\bar{\mu}_{n,i}}\right) f_i N \tag{D3}$$

where

$$1/\bar{\mu}_{n,i} \equiv \sum_{k\geq 1} p_k^{(i)}/k \tag{D4}$$

is the number-average multiplicity of the junction.[31,33] The correction factor for overcounting has changed to $(k-1)/k$. The number-average is then given by

$$P_n^{-1} = 1 - \sum_i f_i (1 - 1/\bar{\mu}_{n,i}) \tag{D5}$$

or equivalently

$$P_n = (1/\sum f_i)/[1/\bar{\mu}_n + 1/\sum f_i - 1] \tag{D6}$$

where the total number-average of the junction multiplicity is defined by

$$1/\bar{\mu}_n \equiv \sum_i (f_i/\bar{\mu}_{n,i})/\sum_i f_i \tag{D7}$$

Let us next introduce a new function

$$u_i(x) \equiv \sum_{k\geq 1} p_k^{(i)} x^{k-1} \tag{D8}$$

for each species i. This function appears in the conventional cascade theory of gelation.[42] It describes the structure of a junction formed by $R\{A_i\}$. The above result for P_n is then written as

$$P_n^{-1} = 1 - \sum_i f_i \int_0^1 x u_i'(x)\, dx \tag{D9}$$

where $u_i'(x)$ is the derivative of $u_i(x)$.

If all reactions are reversible, we have the equilibrium condition

$$[(f_i N) p_k^{(i)}]/[(f_i N) p_1^{(i)}]^k = K_k^{(i)} \tag{D10}$$

for each junction of multiplicity k formed by the ith functional groups, where $K_k^{(i)}$ is the equilibrium constant. Since the following arguments equally hold for all species, let us temporarily drop the cumbersome superscript (i).

As in our previous study[33] for thermoreversible gelation with junctions of variable multiplicity, we next assume that the equilibrium constant takes the form

$$K_k = \lambda(T)^{k-1}\gamma_k \tag{D11}$$

where $\lambda(T)$ is the association constant for a single functional group. It can be written as

$$\lambda(T) = \exp(-\Delta f/k_B T) \tag{D12}$$

in terms of the free energy Δf produced when a functional group is bound into the junction. The factor γ_k gives a surface correction to the free energy due to finite size of the junction. Substituting this form for p_k into the function $u(x)$, we find

$$u(x) = p_1 \tilde{u}(z) \tag{D13}$$

where

$$z \equiv \lambda(T)(fN) p_1 x \tag{D14}$$

is the variable used in our previous study[33] and the function $\tilde{u}(x)$ is the same as the one defined by eq 4.8. The normalization condition $u(1) = 1$ gives

$$\lambda(T)(fN) = z\tilde{u}(z) \tag{D15}$$

The number-average DP can be rewritten as

$$P_n^{-1} = 1 - \sum_i \frac{1}{\lambda_i N} \int_0^{z_i} x \tilde{u}_i'(x)\, dx \tag{D16}$$

Omitting the redundant symbol ˜, we obtain eq B4.

Let us next consider the weight-average P_w. From the number-average, one can easily guess that the weight-average is given by

$$P_w = (1/\sum f_i)/[1/\bar{\mu}_w + 1/\sum f_i - 1] \tag{D17}$$

where the weight-average junction multiplicity is defined by

$$\bar{\mu}_w \equiv \sum_i f_i \bar{\mu}_{w,i}/\sum_i f_i \tag{D18}$$

with the weight-average multiplicity of each species

$$\bar{\mu}_{w,i} \equiv \sum_{k\geq 1} k p_k^{(i)} \tag{D19}$$

In fact, one can easily check this result by the following simple intuitive consideration in the case where there are only two species. Rigorous proof for the general case of arbitrary number of species requires complex mathematical analysis of the cascade process, which we have presented in our recent paper.[43]

Let us consider functional molecules $R\{A_f/B_g\}$ carrying number f of A groups and number g of B groups. These functional groups form junctions of arbitrary multiplicity within the same species. We first consider the clusters that are formed by association of B groups only. A cluster including n molecules carry fn of A

groups. Therefore, their weight-average A-functionality f_w is given by

$$f_w = f \times \frac{gN}{N}\left\{\frac{\bar{\mu}_{w,B} - 1}{1 - (g-1)(\bar{\mu}_{w,B} - 1)} + \frac{1}{g}\right\} \qquad \text{(D20)}$$

according to eqs A.18 and A.24 of Fukui-Yamabe,[31] where $\bar{\mu}_{w,B}$ is the weight-average junction multiplicity of B species. We then introduce association among A groups on these clusters. The weight-average DP is then given by

$$P_w = (1/f)/[1/f_w + 1/\bar{\mu}_{w,A} - 1] \qquad \text{(D21)}$$

which reduces to eq D17 when rearranged.

Acknowledgment. The author would like to thank Professor E. Ogawa for enlightening discussions on the helix formation of gellan gum at finite concentrations. The work is supported by Grant-in-Aid for Scientific Research on Priority Areas (A), "Dynamic Control of Strongly Correlated Soft Materials" (No.413/13031048) from the Ministry of Education, Science, Sports, Culture, and Technology, Japan.

References and Notes

(1) Burchard, W. *Br. Polym. J.* **1985**, *17*, 154.
(2) Clark, A. H.; Ross-Murphy, S. B. *Adv. Polym. Sci.* **1987**, *83*, 57.
(3) Kramer, O. *Biological and Synthetic Polymer Networks*; Elsevier Applied Science: London and New York, 1988.
(4) Guenet, J. M. *Thermoreversible Gelation of Polymers and Biopolymers*; Academic Press and Harcourt Brace Jovanovich Publishers: San Diego, CA, 1992.
(5) Nishinari, K., Doi, E., Eds. *Food Hydrocolloids: Structures, Properties, and Functions*; Plenum Press: New York, 1994.
(6) te Nijenhuis, K. *Adv. Polym. Sci.* **1997**, *130*, 1.
(7) Rochas, C.; Rinaudo, M. *Biopolymers* **1980**, *19*, 1675.
(8) Rochas, C.; Rinaudo, M. *Biopolymers* **1984**, *23*, 735.
(9) Higgs, P. G.; Ball, R. C. *J. Phys. (Paris)* **1989**, *50*, 3285.
(10) Viebke, C.; Piculell, L.; Nilsson, S. *Macromolecules* **1994**, *27*, 4160.
(11) Tanaka, F. *Macromolecules* **2000**, *33*, 4249.
(12) Djabourov, M.; Leblond, J.; Papon, P. *J. Phys. (Paris)* **1988**, *49*, 319; 333.
(13) Berghmans, M.; Thijs, S.; Cornette, M.; Berghmans, H.; De Schryver, F. C.; Moldenaers, P.; Mewis, J. *Macromolecules* **1994**, *27*, 7669.
(14) Buyse, K.; Berghmans, H.; Bosco, M.; Paoletti, S. *Macromolecules* **1998**, *31*, 9224.
(15) Itagaki, H.; Takahashi, I. *Macromolecules* **1995**, *28*, 5477.
(16) Normand, V.; Muller, S.; Ravey, J. C.; Parker, A. *Macromolecules* **2000**, *33*, 1063.
(17) Bongaerts, K.; Reynaers, H.; Zanetti, F.; Paoletti, S. *Macromolecules* **1999**, *32*, 675.
(18) Iliopoulos, I.; Audebert, R. *Eur. Polym. J.* **1988**, *24*, 171; *J. Polym. Sci., Polym. Chem. Ed.*, **1988**, *26*, 275.
(19) Morris, E. R.; Rees, D. A.; Thom, D.; Boyd. J. *Carbohydr. Res.* **1978**, *66*, 145.
(20) Cuppo, F.; Reynaers, H.; Paoletti, S. *Macromolecules* **2002**, *35*, 539.
(21) Poland, D.; Scheraga, H. A. *Theory of Helix-Coil Transitions in Biopolymers*; Academic Press: San Diego, CA, 1970.
(22) Zimm, B. H.; Bragg, J. K. *J. Chem. Phys.* **1959**, *31*, 526.
(23) Lifson, S.; Roig, A. *J. Chem. Phys.* **1961**, *34*, 1963.
(24) Flory, P. J. *J. Chem. Phys.* **1942**, *10*, 51.
(25) Huggins, M. L. *J. Chem. Phys.* **1942**, *46*, 151.
(26) Flory, P. J. *Principles of Polymer Chemistry*; Cornell University Press: Ithaca, NY, 1953.
(27) Koningsveld, R.; Stockmayer, W. H.; Nies, E. *Polymer Phase Diagrams*; Oxford University Press: Oxford, England, 2001.
(28) Flory, P. J. *J. Am. Chem. Soc.* **1941**, *63*, 3091; 3096.
(29) Stockmayer, W. H. *J. Chem. Phys.* **1943**, *11*, 45; **1944**, *12*, 125.
(30) Stockmayer, W. H. *J. Polym. Sci.* **1952**, *9*, 69.
(31) Fukui, K.; Yamabe, T. *Bull. Chem. Soc. Jpn.* **1967**, *40*, 2052.
(32) Tanaka, F. *Macromolecules* **1990**, *23*, 3784; 3790.
(33) Tanaka, F.; Stockmayer, W. H. *Macromolecules* **1994**, *27*, 3943.
(34) Borgström, J.; Quist, P.-O.; Piculell, L. *Macromolecules* **1996**, *29*, 5926.
(35) Borgström, J.; Egermayer, M.; Sparrman, T.; Qest, P.-O.; Piculell, L. *Langmuir* **1998**, *14*, 4935.
(36) Ramzi, M.; Rochas, C.; Guenet, J. M. *Macromolecules* **1996**, *29*, 4668.
(37) Reid, D. S.; Bryce, T. A.; Clark, A. H.; Rees, D. A. *Faraday Discuss. Chem. Soc.* **1974**, *57*, 230.
(38) Morris, E. R.; Rees, D. A.; Robinson, C. *J. Mol. Biol.* **1980**, *138*, 349.
(39) Grasdalen, H.; Smidsrød, O. *Macromolecules* **1981**, *14*, 1845.
(40) Smidsrød, O.; Grasdalen, H. *Carbohydr. Polym.* **1982**, *2*, 270.
(41) Gornick, F.; Jackson, J. L. *J. Chem. Phys.* **1963**, *38*, 1150.
(42) Gordon, M. *Proc. R. Soc. (London)* **1962**, *A268*, 240.
(43) Tanaka, F. To appear in *J. Polym. Sci., Part B: Polym. Phys.*
(44) de Gennes, P. G. *Scaling Concepts in Polymer Physics*; Cornell University Press: Ithaca, NY, 1979.
(45) Tanaka, F.; Koga, T. *Comput. Theor. Polym. Sci.* **2000**, *10*, 259.

MA021688Y